BICOM 93/9 **August 1993**

An adaptive finite element technique with a-priori mesh grading

Th Apel, R Mücke and J R Whiteman

Submitted to Numerical Methods for Partial Differential Equations.

An adaptive finite element technique with a-priori mesh grading

Thomas Apel* Roland Mücke† John R. Whiteman

BICOM, Institute of Computational Mathematics,
Brunel. The University of West London,
Uxbridge, Middlesex, UB8 3PH,
England

August 25, 1993

Abstract. In this paper we discuss a combined a-priori a-posteriori approach to mesh refinement in finite element methods for two- and three-dimensional elliptic boundary value problems containing boundary singularities. We review first both techniques of a-priori mesh grading around singularities and a-posteriori mesh refinement controlled by local error indicators. In examples of two- and three-dimensional boundary value problems we demonstrate the applicability and efficiency of various combined mesh refinement strategies.

Key Words. Elliptic boundary value problem, finite element method, adaptive mesh refinement, a-posteriori error estimation, a-priori mesh grading, singularities.

*Supported by DAAD (German Academic Exchange Service), No. 517/009/511/3.
†Supported by DAAD (German Academic Exchange Service), No. 517/009/503/3.

1 Introduction

The quality of a finite element approximation to the solution of an elliptic boundary value problem can vary markedly over the computational domain. This is particularly the case when boundary singularities, arising from re-entrant corners and edges or from the change of the type of boundary conditions, are present. The deterioration of the approximation arises on account of the lower global regularity of the solutions in these situations as compared with problems having smooth boundaries and only one type of boundary condition. Many special numerical techniques have been developed in recent years to compensate for the effects of these *singularities*, and there is an extensive literature in this field, see e. g. [1]–[14]. In this paper we shall focus on strategies, which are a combination of *a-priori* grading and *a-posteriori* (or adapted) mesh refinement techniques.

The *a-priori* local mesh grading approach has been analyzed mainly in the two-dimensional case [15]–[18], but there are also some studies of three-dimensional contexts, see [1, 2, 3, 7, 8]. Based on analytical knowledge of the solution of the boundary value problem a mesh can be described which will produce optimal *a-priori* error estimates. The only information necessary for this is a lower estimate for the exponent β in the singular part of the solution, for β see (4.1). This technique can be applied with any finite element code. The only modification necessary is in the preprocessor to generate the *a-priori* graded mesh. It can be shown that the number of degrees of freedom for such a mesh is asymptotically the same as for ungraded meshes and that the asymptotic behaviour of the condition number of the resulting finite element stiffness matrix is not worse than that for problems with regular solutions [2, 3, 15, 16]. The disadvantage of the *a-priori* analysis is that it considers only the *asymptotic behaviour* of the finite element solution as the number of degrees of freedom tends to infinity. Nevertheless it is an important part of finite element analysis because it demonstrates the mesh which in this sense is optimal.

However, for detailed knowledge of the errors in a particular finite element approximation and for assessing its acceptability, an *a-posteriori* error estimate has to be provided. Since the first papers by *Babuška* and *Rheinboldt* [19, 20, 21] many different estimators have been developed and included in finite element codes, for a review and comparison see for example [11, 23, 24]. Usually *a-posteriori* error estimates are calculated locally and then amalgamated to form a global error estimate. They can thus also serve as an indicator for regions with large or small errors, respectively, and can

be used to determine where a mesh has to be refined or even where it can be coarsened. This feature has brought a new dimension to finite element analysis, namely the creation of automatic mesh adapting finite element strategies. The process can be described as follows: Starting with a coarse initial mesh, the three steps

- calculating an approximate solution,
- estimating the error locally,
- generating an improved mesh,

are executed repeatedly until the error globally is within a desired tolerance, for example 5% or 10% in engineering applications.

In the h-version of adaptivity, which we consider here, there are two main strategies for improving the mesh. The first is based on a subdivision of the existing elements. This is relatively easy to program, but has the disadvantage, that adjacent elements have only a small number of possible ratios of their mesh sizes, mainly $1:1$ or $1:2$. The second approach demands a complete remeshing on the basis of a mesh density function derived from the error estimator [22, 26] and it is necessary to have an automatic mesh generator working with this background information. In this case the meshes produced have a more gradually changing mesh size.

Especially in the first strategy, even though the sequence of meshes depends strongly on the initial mesh, often little attention is payed to an appropriate design of this mesh. In most cases *a-priori* knowledge of where the errors are large is totally ignored and not exploited in the design of the initial mesh.

The initial question of our investigation is whether savings in computational effort can be achieved by using mesh grading techniques combined with adaptive techniques. As a measure we shall use the number of refinement steps and the number of degrees of freedom required to achieve a finite element solution with an error below a given tolerance.

The outline of the paper is as follows. In Sections 2 and 3 we state the class of problems to be considered and give basic information on the discretizations. In Section 4 we introduce the idea of appropriate mesh design for approximating functions of r^β-type. In a further section we derive an error estimator by using the residuals of the finite element solution. This estimator proves to be equivalent to that of [21]. In Sections 6 and 7 we summarize our computational experiments and finally conclusions are given.

2 The model problem

2.1 Classical formulation

The diffusion or the flow of some quantity such as heat, mass, electric or magnetic charge occurs in a wide range of physical processes. In such situations the gradient of the rate of transfer per unit area, the vector function $\mathbf{q}$, and an appropriate source term f have to satisfy the balance or continuity requirement

$$\nabla \cdot \mathbf{q} = f\,. \tag{2.1}$$

The transport variable $\mathbf{q}$ itself is often related to a scalar potential function u,

$$\mathbf{q} = -\mathbf{K} \cdot \nabla u\,, \tag{2.2}$$

where $\mathbf{K}$ is a symmetric and positive definite tensor of second order whose coefficients K_{ij} describe the character of the physical medium; for example, the thermal conductivity in heat conduction problems, the permeability in electro-static problems, or $\mathbf{K}$ can be just a unit tensor in the case of incompressible flow problems. If the coefficients K_{ij} are constants, i. e. independent of position, the medium is called homogeneous, otherwise it is nonhomogeneous. If $\mathbf{K}$ is only diagonal, we call the medium orthotropic. If further these diagonal elements are all equal, i. e. $K_{ii} = K$ for all $i = 1, \ldots, d$ where d is the dimension of the domain, the medium is said to be isotropic.

With (2.1) and (2.2) the potential function u is characterized by the quasi-harmonic differential equation

$$\Delta^* u + f \equiv \nabla \cdot (\mathbf{K} \cdot \nabla u) + f = 0 \qquad \text{in} \quad \Omega \subset \mathrm{R}^{\mathrm{d}},\ d = 1, 2, 3 \tag{2.3}$$

together with essential and natural boundary conditions

$$u = \overline{u} \quad \text{on} \quad \Gamma_u\,, \tag{2.4}$$

$$-\nabla^* u - \sigma u \equiv -(\mathbf{K} \cdot \nabla u) \cdot \mathbf{n} - \sigma u = \overline{q} \quad \text{on} \quad \Gamma_q\,, \tag{2.5}$$

where $\partial\Omega \equiv \Gamma = \Gamma_u \cup \Gamma_q$ and $\Gamma_u \cap \Gamma_q = \emptyset$. The outward normal unit vector is denoted by $\mathbf{n}$ and σ is a physical constant associated with the transfer through the surface part Γ_q. For convenience in (2.3) and (2.5) we have introduced the two scalar differential operators Δ^* and ∇^*.

Example 2.1 The general equations given above are now interpreted for steady state heat conduction. In this case $\mathbf{K}$ denotes the thermal conductivity of the body under investigation. For an isotropic medium $\mathbf{K}$ is characterized by a scalar K, namely $\mathbf{K} \equiv K\,\mathbf{I}$ where $\mathbf{I}$ is a second order unit tensor. The potential function u denotes the temperature distribution and the transport variable $\mathbf{q}$ stands for the heat flow within the body. The relation between the heat flow and the temperature gradient is given by *Fourier*'s law of heat conduction, represented in (2.2). On the boundary either the surface temperature, u, or the heat flow, here defined as heat outflow, normal to the surface part, $q_n = \overline{q} + \sigma u$ with $q_n = -\nabla^* u$, is prescribed. In particular, with $\sigma = 0$ and $\overline{q} = 0$ we get the condition for an ideal thermal isolated surface, i. e. $\nabla^* u = 0$. With $\overline{q} = -\sigma u_0$ where σ is the thermal conductance and u_0 is the reference temperature outside the domain *Newton*'s law of cooling is represented as $q_n = \sigma(u - u_0)$.

Let $\Omega^* \subseteq \Omega$ be an arbitrary control volume and $\Gamma^* = \partial\Omega^*$ its surface. The *Gauss* theorem

$$\int_{\Omega^*} \Delta^* u \, d\Omega = \int_{\Gamma^*} \nabla^* u \, d\Gamma \,, \tag{2.6}$$

or expressed using (2.3) and (2.5) by

$$\int_{\Omega^*} f \, d\Omega = \int_{\Gamma^*} q_n^* \, d\Gamma \tag{2.7}$$

where q_n^* denotes the heat transport normal to the surface Γ^*, indicates the local and global equilibrium of heat flow.

2.2 Weak formulation of the boundary value problem

Because of the second order derivatives in the differential operator the classical formulation of the boundary value problem requires at least that $u \in C^2(\Omega) \cup C^1(\Omega \cup \Gamma_q) \cup C^0(\overline{\Omega})$ and $K_{ij} \in C^1(\Omega) \cup C^0(\Omega \cup \Gamma_q)$. In practical applications, however, the coefficients K_{ij} are often discontinuous, for example piecewise constant, so that the classical derivatives at points of discontinuity are not defined. In order to overcome this and to make possible the use of finite element methods, a weaker formulation of the boundary value problem is set up. To obtain this we multiply the equilibrium conditions by an arbitrary test function and integrate over Ω and Γ_q so that

$$\int_{\Omega} (\Delta^* u + f)\, v \, d\Omega - \int_{\Gamma_q} (\nabla^* u + \sigma u + \overline{q})\, v \, d\Gamma = 0 \quad \forall v \in V \tag{2.8}$$

where $V = \{v \in H^1(\Omega), v = 0 \text{ on } \Gamma_u\}$ denotes the *Hilbert* space of functions with square-integrable first derivatives and homogeneous conditions on Γ_u. Employing *Green*'s theorem in the form

$$\int_\Omega v\, \Delta^* u\, d\Omega = \int_\Gamma v\, \nabla^* u\, d\Gamma - \int_\Omega \nabla v \cdot \mathbf{K} \cdot \nabla u\, d\Omega \tag{2.9}$$

we obtain the weak formulation of the boundary value problem as follows: Find an $u \in \overline{V}$ such that

$$a(u, v) = b(v) \qquad \forall\, v \in V\,. \tag{2.10}$$

Here we have introduced the following notation: $\overline{V} = \{u \in H^1(\Omega), u = \overline{u}$ on $\Gamma_u\}$ is the set of functions with square-integrable first derivatives that satisfy the boundary condition on Γ_u, $a(.,.)$ and $b(.)$ are bilinear and linear forms defined on $H^1 \times H^1$ and H^1, respectively,

$$a(u, v) = \int_\Omega \nabla u \cdot \mathbf{K} \cdot \nabla v\, d\Omega + \int_{\Gamma_q} \sigma\, u\, v\, d\Gamma \tag{2.11}$$

$$b(v) = \int_\Omega f\, v\, d\Omega - \int_{\Gamma_q} \overline{q}\, v\, d\Gamma\,. \tag{2.12}$$

Notice, that $\|.\|_E \equiv \sqrt{a(.,.)}$ defines the energy norm on V, provided that the problem has an unique solution. This is satisfied for $\Gamma_u \neq \emptyset$ or $\sigma \neq 0$. Otherwise a solution exists and can be determined up to a constant only if the given quantities f in Ω and q_n on Γ are in equilibrium.

2.3 Singular solutions for two- and three-dimensions

The regularity of the solution of problem (2.3–2.5) or (2.10–2.12) is determined by the smoothness of the coefficients K_{ij} and the right-hand sides f, $\overline{u}$, and $\overline{q}$, as well as by the properties of the domain. For sufficiently smooth domains and coefficients the so-called shift theorem holds; that means, that for $k \geq 0$

$$u \in H^{k+1}(\Omega) \quad \text{if} \quad f \in H^{k-1}(\Omega),\ \overline{q} \in H^{k-1/2}(\Gamma_q),\ \overline{u} \in H^{k+1/2}(\Gamma_u)\,.$$

This is no longer true, when the domain Ω contains corners in two dimensions or corners or edges in three dimensions. We summarize here results on singularities, see e. g. [25, 28] and the references therein.

Consider first two dimensional problems and for simplicity smooth data; we let K_{ij}, $f \in C^\infty(\Omega)$, and σ, $\overline{q}$, $\overline{u}$ be traces of $C^\infty(\Omega)$-functions with

respect to Γ_q and Γ_u, respectively. Further let Ω be a two-dimensional domain and consider one boundary point $\mathbf{x}_0$ which is a re-entrant corner, or a point at which the type of the boundary condition changes. Denote by ω the internal angle at this point.

Introduce polar co-ordinates (r, φ) in the neighbourhood $U = \{\mathbf{x} \in \mathrm{R}^2 : |\mathbf{x} - \mathbf{x}_0| \leq R_0\}$. For convenience consider r as dimensionless, for example say that r is the distance to the corner divided by R_0. In this case the solution u can in general be represented by

$$u = \xi(r) \sum_i \gamma_i r^{\beta_i} \Phi_i(\varphi) + u_r \,. \tag{2.13}$$

The constants γ_i are called stress intensity factors, $\xi(.)$ is a cut-off function ($\xi(r) = 1$ for $r < \frac{1}{2}$, $\xi(r) = 0$ for $r > 1$, $\xi(.) \in C^\infty[0, \infty)$), $\Phi_i(.)$ are smooth (in general trigonometric) functions of the polar angle, $\beta_i \in (0, 1)$ are real numbers, and u_r is the regular part of the solution.

Remark 2.2 The number of terms in the sum in (2.13) is mainly influenced by the desired smoothness of the regular part u_r. If we require $u_r \in H^2(\Omega)$, then the sum reduces to one term in the following cases:

(a) The type of the boundary condition does not change at the point $\mathbf{x}_0$, and $\pi < \omega < 2\pi$.

(b) The type of the boundary condition changes at $\mathbf{x}_0$, and $\omega_1 < \omega < \omega_2$. The angles $\omega_1 < \pi$ and $\omega_2 > \pi$ are determined by the coefficients K_{ij}. For the *Laplace* operator it is $\omega_1 = \frac{\pi}{2}$ and $\omega_2 = \frac{3\pi}{2}$.

For $\omega < \pi$ in (a) and $\omega < \omega_1$ in (b) it follows that $u \in H^2(\Omega)$, which means that we have no singularity. For $\omega > \omega_2$ in (b) there are two singular terms.

Remark 2.3 There are some exceptional angles which depend on the coefficients K_{ij}. In these cases the representation formula (2.13) is not valid, and additional logarithmic terms must be included.

Remark 2.4 The exponents β_i are solutions of an eigenvalue problem but they are in two dimensions known exactly: for the *Laplace* operator we have $\beta = \frac{\pi}{\omega}$ in case (a) of Remark 2.2, in case (b) there is $\beta_1 = \frac{\pi}{2\omega}$ and $\beta_2 = \frac{3\pi}{2\omega}$ (if $\omega > \frac{3\pi}{2}$).

In three dimensions, the irregular boundary points are classified as conical corners, edges and polyhedral corners, and there is an extensive literature about the regularity of the solutions in these cases; we mention here only the books of *Grisvard* [25] and *Kufner/Sändig* [28]. The regularity results can be summarized in the following way:

Near conical points the solution u behaves as in the two-dimensional case, r is here the distance to the corner. The only difference is that the functions Φ_i depend now on two spherical co-ordinates and the exponents β_i cannot in general be determined exactly. In this case

$$u = \xi(r) \sum_i \gamma_i r^{\beta_i} \Phi_i(\varphi, \theta) + u_r \,. \tag{2.14}$$

Near edges we have also a representation formula similar to (2.13). Here, r is the distance to the edge, but the coefficients γ_i are no longer constants. Denote by z the co-ordinate in direction of the edge, then

$$u = \xi(r) \sum_i \gamma_i(z) r^{\beta_i} \Phi_i(\varphi) + u_r \tag{2.15}$$

holds, assuming that the angle of the edge is constant and that in (2.3–2.5) we consider constant coefficients K_{ij}. The exponents β_i are as in the two-dimensional case, see Remark 2.4.

In the case of polyhedral corners we have a superposition of corner and edge singularities. The additional difficulty is that the functions $\Phi_i(\varphi, \theta)$ of the spherical co-ordinates are no longer smooth. We remark that this situation gets still more complicated when the data is not smooth and more general edges are considered. These problems are excluded here.

3 The finite element discretization

3.1 The finite element method as projection technique

We assume that the domain Ω can be represented (exactly or approximately) by an union of m finite elements $\overline{\Omega}_i$, i. e.

$$\overline{\Omega} = \cup_{i=1}^{m} \overline{\Omega}_i \,, \quad \Omega_i \cap \Omega_j = \emptyset \quad \text{for} \quad i \neq j \,. \tag{3.1}$$

We only consider so-called regular finite element meshes in which each node of an element corresponds to a node of the adjacent element. We define a set of C^0-continuous shape functions $\overline{V}^h = \text{span}\{N_i\}_{i=1}^n$ where n denotes the

total number of nodes. In conforming finite element techniques considered here the finite element set is a subset of $\overline{V}$, i. e. $\overline{V}^h \subset \overline{V}$. Thereby the weak formulation of the boundary value problem is projected into finite dimensions as follows: Find $u^h \in \overline{V}^h$ such that

$$a(u^h, v^h) = b(v^h) \qquad \forall\, v^h \in V^h\,. \tag{3.2}$$

The difference between the finite element solution u^h and the exact solution u is represented by the error function $e = u - u^h$. Notice, that the error function becomes homogeneous on Γ_u and we can write

$$\|e\|_E^2 = a(e,e) = b(e)\,. \tag{3.3}$$

From (2.10) and (3.2) we derive the orthogonality relation of the projection

$$a(u - u^h, v^h) = a(e, v^h) = 0 \qquad \forall\, v^h \in V^h, \tag{3.4}$$

i. e. in the $a(.,.)$ product the error function e is orthogonal to the discrete test space V^h. This implies that the finite element method as a projection method gives the best global energy approximation with respect to the underlying finite element space. In addition it turns out that the discretization error is represented as energy difference

$$b(e) = b(u) - b(u^h) = a(u,u) - a(u^h, u^h) = a(e,e)\,. \tag{3.5}$$

Assume the exact solution u can be represented by $u = w + u_0$ where $w \in V$ satisfies the homogeneous essential boundary condition and u_0 with $u_0 = \overline{u}$ on Γ_u is employed to fulfil the nonhomogeneous condition. The weak formulation can then be rewritten as

$$a(w, v) = b^*(v) \qquad \forall\, v \in V \tag{3.6}$$

where $b^*(v) \equiv b(v) - a(u_0, v)$. Notice, that $\sqrt{a(w,w)}$ is now the energy norm of w.

Suppose the surface function $\overline{u}$ can be exactly represented by the finite element interpolation, i. e. $\overline{u} = \overline{u}^h$ on Γ_u. Let $\overline{u}_i$ be prescribed boundary values at the n_u surface nodes on Γ_u then an appropriate function u_0 is given as $u_0 = u_0^h = \sum_{i=1}^{n_u} N_i\, \overline{u}_i$. The finite element spaces are now $\overline{V}^h = V^h + \sum_{i=1}^{n_u} N_i\, \overline{u}_i$ and $V^h = \mathrm{span}\{N_i\}_{i=1}^{N}$ where N denotes the number of degrees of freedom of the finite element discretization, that means the number of nodes in $\overline{\Omega}$ reduced by the number of nodes on Γ_u.

3.2 Extrapolation techniques

It is well known that in a sequence of sufficiently fine finite element meshes the energy global error has the asymptotic behaviour

$$\|e\|_E^2 = \|u - u^h\|_E^2 \approx C^* N^{-\alpha} . \tag{3.7}$$

Here, α is the convergence order of the finite element solution, N the number of degrees of freedom of the finite element discretization, and C^* denotes a constant which is independent of N but dependent on the solution domain, the regularity of the exact solution, the polynomial order of the finite element shape functions and the mesh geometry [29]. An *a-priori* calculation or estimation of the constant C^* is usually impossible. Therefore the *a-priori* estimate (3.7) describes the *behaviour* of the global discretization error but cannot be applied to determine a specific error level for the finite element solution.

The energy convergence order for a sequence of uniformly refined meshes is given by

$$\alpha = \frac{2}{d} \min(s-1, p) \tag{3.8}$$

where d is the dimension of the problem considered, s is the highest order of the *Sobolev* space which contains the exact solution and p denotes the polynomial order of shape functions [29]. Obviously, in problems with singularities in the gradient of the solution, i. e. $s < 2$, the convergence order is determined by the regularity s of the exact solution. Also the inverse theorem is valid, i. e. an observed numerical convergence in the energy of order α indicates a certain smoothness of the exact solution of the boundary value problem [29].

Expression (3.7) can be represented on a double logarithmic scale as the straight line

$$\ln\|e\|_E^2 = -\alpha \ln N + \ln C^* \tag{3.9}$$

where α is the gradient. If we assume the convergence behaviour is already in the asymptotic range so that (3.7) has become valid, then using three finite element meshes we can extrapolate the unknown energy $a(u,u)$ of the exact solution, the constant C^* and the convergence order α by the three equations

$$a(u,u) - a(u_1^h, u_1^h) \;=\; C^* N_1^{-\alpha} ,$$

$$
\begin{aligned}
a(u,u) - a(u_2^h, u_2^h) &= C^* N_2^{-\alpha}, \\
a(u,u) - a(u_3^h, u_3^h) &= C^* N_3^{-\alpha}.
\end{aligned}
\tag{3.10}
$$

If we estimate the convergence order either *a-priori* by (3.8) where the regularity of the exact solution has to be known or *a-posteriori* by error estimators η which should have asymptotically the same convergence rate as the energy,

$$
\alpha \approx \frac{\ln \eta_1^2 - \ln \eta_2^2}{\ln N_2 - \ln N_1}, \tag{3.11}
$$

we can reduce the number of finite element meshes to two. The extrapolated energy $a_{\mathrm{ex}}(u,u) \approx a(u,u)$ is then given by

$$
a_{\mathrm{ex}}(u,u) = \frac{a(u_1,u_1) - a(u_2,u_2)\left(\frac{N_2}{N_1}\right)^{\alpha}}{1 - \left(\frac{N_2}{N_1}\right)^{\alpha}}. \tag{3.12}
$$

4 A-priori mesh grading

In this section, we want to motivate mesh grading and derive the relation between the element sizes and their distance from the point of boundary singularity. For this we adopt the notation from Section 2.3 and consider for simplicity a two-dimensional problem with a solution which has a regular part $u_r \in H^2(\Omega)$ and only one singular term (see Remark 2.2), so that the solution u can be represented by

$$
u = \gamma\, \xi(r) r^{\beta} \Phi(\varphi) + u_r. \tag{4.1}
$$

We now follow the idea of *Oganesyan* and *Rukhovets* [30] and consider the co-ordinate transformation

$$
r^{\mu} = \varrho, \quad \mu \in (0,1].
$$

That means that the neighbourhood $U = \{(x,y) \in \Omega : r \equiv (x^2+y^2)^{1/2} < 1\}$ is transformed into itself, but the singular part of the solution is now

$$
u_s = u_s(\varrho,\varphi) = \gamma \bar{\xi}(\varrho) \varrho^{\beta/\mu} \Phi(\varphi). \tag{4.2}
$$

The advantage is that, in contrast to $\dfrac{\partial u_s}{\partial r}$, the derivatives $\dfrac{\partial^k u_s}{\partial \varrho^k}$ $(k = 1,2,\ldots)$ are bounded for sufficiently small values of μ $(\mu \le \frac{\beta}{k})$. We can suppose that

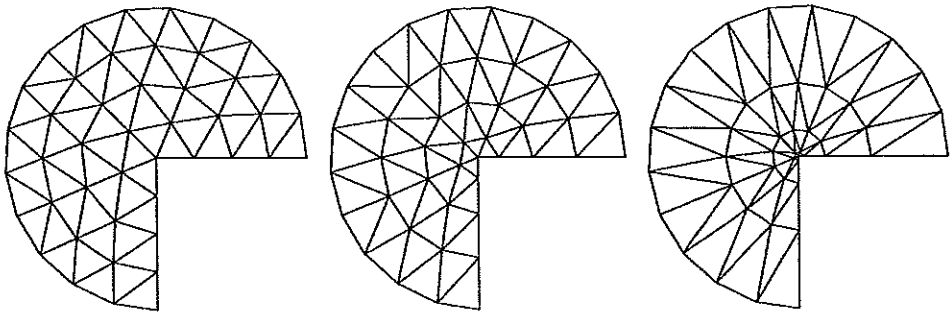

Figure 4.1: Mesh in the transformed plane (ϱ, φ) (left); graded mesh in the original (r, φ) plane, $\mu = 0.7$ (middle); graded mesh in the original (r, φ) plane, $\mu = 0.4$ (right).

u_s can be approximated on a typical quasiuniform mesh of element size h with optimal order (depending on the degree of the shape functions).

Trying to avoid this co-ordinate transformation for practical calculations (for example one would have to transform also the input data) has led to the idea of creating only the mesh in the transformed domain, of transforming back immediately and of computing on the transformed mesh but in the original co-ordinate system. Two examples of transformed meshes are given in Figure 4.1.

In the following, we want to derive another description of the graded mesh so constructed in the original co-ordinates. We try to find a relation between the diameter h_i of an element Ω_i and its distance r_i from the corner point.

Elements with a vertex at the corner of the domain are contained in the transformed domain in a circle with the radius $\varrho = h$, which means in the original domain

$$h_i = h^{1/\mu} \quad \text{if} \quad r_i = 0. \tag{4.3}$$

For elements without a vertex at the corner we find a circular annulus that contains the element and has an inner radius ϱ_i and an outer radius ϱ_o such that $\varrho_o - \varrho_i = h$. In the same way we can write for the original domain $r_o - r_i = h_i$, $r_o^\mu = \varrho_o$, $r_i^\mu = \varrho_i$. Consequently, we have

$$\frac{h}{h_i} = \frac{r_o^\mu - r_i^\mu}{r_o - r_i} = \mu r_*^{\mu-1}$$

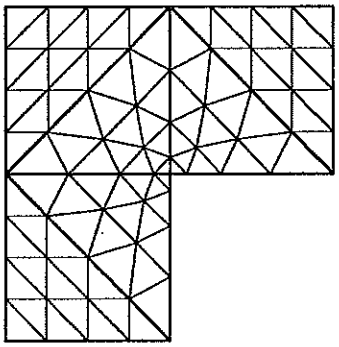

Figure 4.2: Mesh as proposed by *Raugel.*

with some $r_* \in (r_i, r_o)$. This relation can be rewritten in the form $h_i = \frac{1}{\mu} h r_*^{1-\mu}$. Because

$$r_i < r_* < r_o = \varrho_o^{1/\mu} \leq (2\varrho_i)^{1/\mu} = 2^{1/\mu} r_i \tag{4.4}$$

we get $\frac{1}{\mu} h r_i^{1-\mu} < h_i < 2^{-1+1/\mu} \cdot \frac{1}{\mu} h r_i^{1-\mu}$. This means that we demand

$$C_1 h r_i^{1-\mu} \leq h_i \leq C_2 h r_i^{1-\mu} \quad \text{if} \quad r_i > 0. \tag{4.5}$$

The conditions (4.3) and (4.5) are actually those which are used in the proofs for *a-priori* error estimates for graded meshes and are also convenient for verifying whether or not a given mesh generation strategy provides the desired meshes.

A slightly different mesh generation algorithm including a transformation is presented by *Raugel* [16]. Starting with a coarse mesh she divides each triangle into M^2 smaller ones where M is the number of *layers.* The triangles are chosen to be congruent if the initial triangle has no vertex at the critical corner of the domain, and graded otherwise, see Figure 4.2. In fact, this is an approximation of our circular neighbourhood of the corner by a polygonal one.

Another approach is the so-called dyadic partition [7]. Again starting with a coarse mesh the elements are simply divided as in many adaptive refinement strategies, until the conditions (4.3) and (4.5) are fulfilled with suitable constants C_1 and C_2.

We also suppose that one can define a corresponding mesh density function for using a mesh generator of the type described in [22, 26].

Remark 4.1 Adjacent elements are of comparable size. This follows from (4.4) and (4.5). Consequently, there is no difficulty with fulfilling the condition that the aspect ratio of the elements (the ratio between the radius of the smallest outer and the largest inner balls) should be bounded. Note also, that elements in different parts of the domain may not be of comparable size, see (4.3).

Remark 4.2 Our construction of the graded meshes shows that the number of elements is independent of the parameter μ. It can even be shown that the conditions (4.3) and (4.5) yield an asymptotic number of elements of order h^{-2} independently of the manner of construction [3].

Remark 4.3 The asymptotic order of the condition number of the stiffness matrix does not increase when using mesh grading [3, 15].

Remark 4.4 Estimates of the discretization error are derived from different points of view in several papers including [3, 7, 8, 15, 16, 17, 18, 25, 30]. Whilst the proofs are given only for special cases, it can be conjectured that for

$$\mu \leq \mu_* \equiv \frac{\beta}{p} \tag{4.6}$$

the approximation order in *Sobolev* spaces $H^k(\Omega)$ is the same as for problems with the same smoothness of the data in domains with smooth boundaries and without changing type of the boundary conditions. Here, we denote by p the degree of the shape functions.

The extension of mesh grading approach to problems in three-dimensional domains is natural using tetrahedral elements; consider for example a polyhedron with singularities near edges and corners. However, near edges the idea of transformation, mesh generation and re-transformation leads to anisotropic finite elements, see Figure 4.3. According to [1], an element is called *anisotropic* if its diameters in different directions have different asymptotic scales.

Though not fulfilling the condition of a bounded aspect ratio (for elements near the edge the aspect ratio is of the order $h^{1-1/\mu}$), such meshes can be applied successfully, see for instance [1]. One has only to take care that the angles between the faces of each tetrahedron do not tend to π for

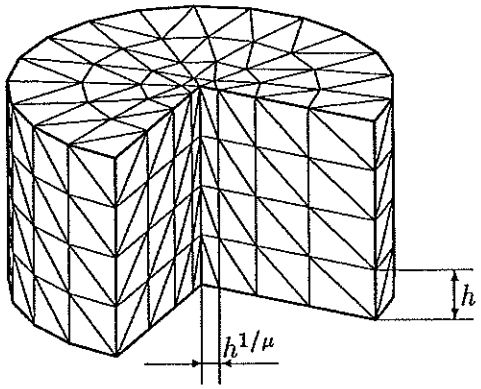

Figure 4.3: Anisotropic, graded mesh near an edge.

decreasing h, but are bounded by some constant $\gamma_* < \pi$, which is independent of the mesh size. For linear elements and some smoothness assumptions on the data, it is shown that the optimal convergence order in the sense of Remark 4.4 is received for

$$\mu \leq \beta.$$

One can expect that this result extends to shape functions of higher degree in the sense of Remark 4.4, but as far as we know, no comprehensive mathematical investigation of anisotropic meshes has yet been done.

On the other hand, describing the mesh by conditions (4.3) and (4.5) it is also possible to consider meshes with bounded aspect ratio. They can be constructed for instance by the method of dyadic partition, see above. Approximations on such meshes are more comprehensively investigated [2, 3, 7, 8] and most of the *a-priori* error estimates from the two-dimensional case are shown to also hold true in three dimensions. There is, however, one serious drawback: the number of elements as well as the condition number of the stiffness matrix increase asymptotically for $\mu \leq \frac{1}{3}$ [2, 3]. This can lead to instability in the computation.

5 A-posteriori error estimation

5.1 Basic features of a-posteriori error estimates

Several techniques of *a-posteriori* error estimation have been elaborated and, based on the number of papers published on this field, it is clear that there has been a dramatic development during the last few years. In order to characterize established error estimators for elliptic boundary value problems we may consider two classes; the residual type and the recovery type of *a-posteriori* error estimation.

The residual type, mainly connected with the works of *Babuška* and his co-workers, uses the duality between the classical and the weak formulation of the boundary value problem [6, 10, 19, 20, 21, 31, 32, 35]. The finite element solution satisfies the weak formulation but in the classical form of the boundary value problem it causes residuals in the equilibrium conditions which are a measure of the discretization error of the finite element solution.

The recovery type of error estimation, based on an idea of *Zienkiewicz* and *Zhu*, uses the difference between the classical finite element solution and a solution which has been improved by recovery techniques [33, 34, 36, 37, 38]. In engineering practice both the residual type and the recovery type estimators are widely applied in complex structural calculations. It is well known that both estimators show qualitatively the same results. Further it has been proved that for uniform meshes of bilinear rectangles both estimators are equivalent from an analytical point of view [27].

We now summarize briefly some basic features of *a-posteriori* error estimation. We shall then apply the residual type of error estimator in the context of general quasi-harmonic boundary value problems and by numerical experiments which are demonstrated in Section 6 and Section 7 we discuss the combined use of *a-priori* mesh grading techniques and *a-posteriori* error control.

A quantity λ_i which estimates the local discretization error in a subdomain, which we take to be the individual element Ω_i, is called the error indicator. The totality of λ_i indicates the distribution of the discretization error in the solution domain. The global error measure, called error estimator η, is related to the local indicators by

$$\eta^2 = \sum_{i=1}^{m} \lambda_i^2 \tag{5.1}$$

where m denotes the number of elements in the total domain. We also

introduce the percentage error of the energy norm by

$$\eta_{\%} = \frac{\eta}{\sqrt{a(u,u)}} \cdot 100\% \tag{5.2}$$

where the global energy is approximated by $a(u,u) \approx a(u^h,u^h) + \eta^2$. The true error $\|e\|_E$ has to be bounded by the error estimator η such that

$$C_1\eta \leq \|e\|_E \leq C_2\eta \tag{5.3}$$

where the constants C_1 and C_2 are independent of the finite element mesh and the exact solution. When C_1 and C_2 are close to unity the estimator η gives the correct error level and the so-called effectivity index, defined by

$$\Theta = \frac{\eta}{\|e\|_E}, \tag{5.4}$$

approaches one as the exact error $\|e\|_E$ tends to zero. If $\Theta \to 1$ the error estimator η is said to be asymptotically exact.

5.2 A residual type error estimator

We consider the linear elliptic boundary value problem (2.3–2.5) and apply a conforming finite element technique to the weak form (2.10). Whilst the essential boundary condition on Γ_u is automatically satisfied by restriction of the bilinear form of the weak formulation over $\overline{V} \times V$, in the equilibrium conditions (2.3) and (2.5) the finite element solution u^h usually leads to residual terms. In a formal sense we can write

$$\Delta^* u^h + f = R + J_{\Gamma_{ij}} \quad \text{in } \Omega \tag{5.5}$$

$$u^h = \overline{u} \quad \text{on } \Gamma_u \tag{5.6}$$

$$-\nabla^* u^h - \sigma u^h = \overline{q} + \xi \quad \text{on } \Gamma_q \tag{5.7}$$

where R denotes the residual distributed in Ω and ξ is the residual along the boundary part Γ_q. The residual term $J_{\Gamma_{ij}}$, for convenience denoted henceforth by J, where

$$J = (\mathbf{K}_i \cdot \nabla u^h) \cdot \mathbf{n}_i + (\mathbf{K}_j \cdot \nabla u^h) \cdot \mathbf{n}_j \tag{5.8}$$

is only defined on the interfaces Γ_{ij} between two elements Ω_i and Ω_j, see Figure 5.1. The residual J represents a weak form, also called generalized

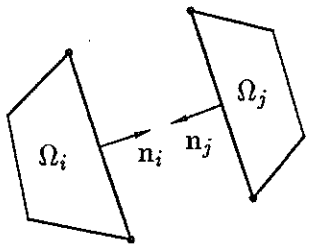

Figure 5.1: Interface between two adjacent elements Ω_i and Ω_j.

form, of the second derivatives of the differential operator with respect to the C^0-continuous finite element approximation.

If we interpret the residuals R, J and ξ as additional loads, the finite element solution u^h can be considered as the exact solution of the *finite element boundary value problem* (5.5–5.7). Both boundary value problems (2.3–2.5) and (5.5–5.7) differ by their loadings and these differences indicate the discretization error of the finite element solution.

Because the flow balance expressed by the *Gauss* theorem has to be satisfied in both the original and the finite element boundary value problem the residuals R, J, and ξ have to be in local and global equilibrium.

Using the linearity in the governing equations we get a boundary value problem for the error function e such that

$$\Delta^* e + R + J = 0 \quad \text{in} \quad \Omega \tag{5.9}$$

$$e = 0 \quad \text{on} \quad \Gamma_u \tag{5.10}$$

$$\nabla^* e + \sigma e = \xi \quad \text{on} \quad \Gamma_q\,. \tag{5.11}$$

In comparison to the original formulation (2.3–2.5) the loads f and $\overline{q}$ are now replaced by the residuals R, J, and ξ. Notice, that the essential boundary condition (5.10) becomes homogeneous.

The boundary value problem of the error function can be represented by its weak formulation. Using the same procedure as in Section 2.2 we get

$$a(e,v) = b(v) \qquad \forall v \in V \tag{5.12}$$

where

$$a(e,v) = \int_\Omega \nabla e \cdot \mathbf{K} \cdot \nabla v \, d\Omega + \int_{\Gamma_q} \sigma \, e \, v \, d\Gamma \tag{5.13}$$

$$b(v) = \int_\Omega R\, v \, d\Omega + \int_{\sum_{\Gamma_{ij}}} J \, v \, d\Gamma + \int_{\Gamma_q} \xi \, v \, d\Gamma\,, \tag{5.14}$$

see also Remark 5.1. Because of the homogeneous boundary condition on Γ_u the bilinear form is now restricted to $V \times V$. Therefore the arbitrary function v can be replaced by the error function and we can write with (3.3) and (5.12–5.14)

$$\|e\|_E^2 = a(e,e) = \int_\Omega R\, e\, d\Omega + \int_{\sum \Gamma_{ij}} J\, e\, d\Gamma + \int_{\Gamma_q} \xi\, e\, d\Gamma\,. \tag{5.15}$$

With (5.15) the global discretization error in the energy norm is represented by the residuals of the finite element solution and the unknown error function e.

In order to get local error indicators which characterize the discretization error of an individual element we have to determine the part of the global discretization error associated with each element. The divisions of the residuals R and ξ into element contributions are obvious. On the interelement surface Γ_{ij} the residual J is shared by two adjacent elements. A division according to $J = J_i + J_j$ with $J_i = (1-c)\,J$ and $J_j = c\,J$ is controlled by the function c which can be achieved iteratively so that in addition to the global equilibrium of residuals, which is satisfied automatically, the local equilibrium is also fulfilled [39, 40]. In a simpler and cheaper way one half of the residual can be allocated to each of the two adjacent elements so that $c = 1/2$. For the contribution of element Ω_i to the total energy error we can now write

$$\|e\|_{\Omega_i}^2 = \int_{\Omega_i} R\, e\, d\Omega + \frac{1}{2}\sum_j \int_{\Gamma_{ij}} J\, e\, d\Gamma + \int_{\Gamma_q \cap \overline{\Omega}_i} \xi\, e\, d\Gamma \tag{5.16}$$

where index j runs over the interelement surfaces of element Ω_i. Finally the element error (5.16) is estimated by [10, 19, 20, 21, 31, 32, 35]

$$\lambda_i^2 = \frac{C^2}{E(\mathbf{K}_i)} \left(h_i^2 \int_{\Omega_i} R^2\, d\Omega + h_i \int_{\partial\Omega_i} \overline{J}^{\,2}\, d\Gamma \right) \tag{5.17}$$

with

$$\overline{J} = \begin{cases} 0 & \text{on } \overline{\Omega}_i \cap \Gamma_u\,, \\ \xi & \text{on } \overline{\Omega}_i \cap \Gamma_q\,, \\ \frac{1}{2} J & \text{on } \overline{\Omega}_i \cap \overline{\Omega}_j\,. \end{cases} \tag{5.18}$$

Here, parameter h_i characterizes the element size, C is a global constant which we estimate by extrapolation techniques, and $E(\mathbf{K}_i)$ denotes the largest eigenvalue of tensor $\mathbf{K}$ which can vary from element to element.

Remark 5.1 Because of the orthogonality relation (3.4) of the finite element projection we cannot solve the boundary value problem of the error function (5.9–5.11) with the same finite element space as the original problem. Assume that the error function can be expressed as a series

$$e = \sum_{i=p+1}^{\infty} N_{(i)}$$

where $N_{(i)}$ is the set of shape functions of order i. Assume further that the leading term in the error series represents globally and locally the discretization error. The difference between a finite element solution of order p and $p+1$ can then be employed for indicating the discretization error. In principle this technique is included in error estimators using smoothing techniques where the discontinuous gradient of the solution is improved by an approximation of higher order.

Remark 5.2 The element error indicator employs both the distributed residual R and the residual $\overline{J}$ on the element surfaces. Both parts of the error indicator are of same order. In finite element approximations with linear shape functions, however, the surface term is dominant so that in an error estimation the residual R can be neglected [10].

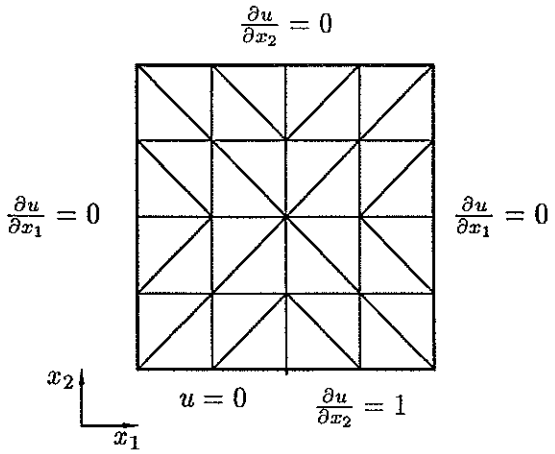

Figure 6.1: The two-dimensional test problem with the initial finite element mesh (domain: 100×100).

6 Mesh grading and adaptivity in two-dimensional problems

6.1 Test example and plan of experiments

We consider first the two-dimensional *Laplace*'s equation, $\Delta u = 0$, together with boundary conditions illustrated in Figure 6.1. The change of the type of boundary condition on the lower surface of the domain causes a singularity in the gradient of the solution of order $O(r^{-\frac{1}{2}})$, see also Subsection 2.3. The discretization error of the finite element solution based on the mesh shown in Figure 6.1 is expected to be significant near this singular point. In order to reduce the discretization error we treat the domain around the singularity with an appropriate mesh refinement. In the next sections we discuss and compare the following strategies of refinement:

- uniform mesh refinement,
- uniform mesh refinement with mesh grading,
- adaptive mesh refinement,
- adaptive mesh refinement with mesh grading.

In uniform mesh refinement each element is subdivided in four elements as illustrated in Figure 6.2, Algorithm A. Obviously, this strategy is not

very powerful because both the *a-priori* information about the exact solution around the singularity and the *a-posteriori* estimation of the discretization error distribution of the finite element solution are not included in this procedure. Mesh grading techniques as discussed in Section 4 make use of the known order of singularity to improve *a-priori* the mesh design. In contrast to *a-priori* mesh grading adaptive mesh refinements are controlled *a-posteriori* by estimating the distribution of the discretization error of the finite element solution. Based on this only those elements in which the estimated error is high are treated with refinement Algorithm A. In order to produce regular meshes a transition between the refined and the unrefined subdomains is realized by subdivision of elements in two as shown in Figure 6.2, Algorithm B.

6.2 Extrapolation of the energy using uniform mesh refinement

We consider first the behaviour of the error estimator η for a sequence of uniformly refined meshes. The one-dimensional discretization parameter h_i in (5.17) is taken as

$$h_{ij} = \text{meas}(\partial\Omega_i)_j \tag{6.1}$$

where $(\partial\Omega_i)_j$ denotes the interface between two adjacent elements Ω_i and Ω_j. For a further discussion concerning h_i see also Section 7. Note that in the example investigated the residual part R of the error estimator disappears. With $E(\mathrm{K}_i) = 1$ for *Laplace*'s equation we get

$$\eta^2 = \sum_{i=1}^{m} \lambda_i^2 = C^2 \sum_{i=1}^{m} \sum_{j=1}^{3} h_{ij} \int_{(\partial\Omega_i)_j} \overline{J}^2 \, d\Gamma \,. \tag{6.2}$$

For the time being the global constant C, which influences the error level but not its distribution, is unity.

The numerical results are summarized in Table 6.1. According to (3.8) the theoretical convergence order of the discretization error becomes $\alpha = \frac{1}{2}$ for the problem illustrated in Figure 6.1. Using (3.11) the convergence order is well represented by the global error estimators for example we get $\alpha = 0.4904$ with the error estimates of the meshes 4 and 5. The error level with $C = 1$, however, is significantly overestimated so that the error level has to be scaled by estimating an appropriate C. Using extrapolation (3.12)

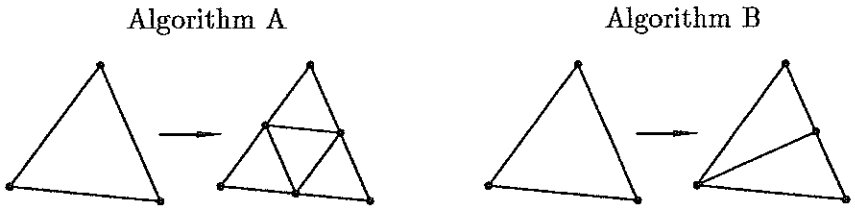

Figure 6.2: Refinement algorithms.

N	$\eta_{C=1}$	$a(u^h,u^h)/10^3$	C	$\eta_\%$
22	38.93	1.411	0.727	60.20 %
76	31.60	1.790	0.651	43.72 %
280	23.63	1.996	0.623	31.31 %
1072	17.14	2.103	0.612	22.29 %
4192	12.27	2.157	0.610	15.91 %

Table 6.1: Uniform refinement: extrapolation of the scale factor C.

we determine the extrapolated energy as $a_{\text{ex}}(u,u) \approx 2.213 \cdot 10^3$. Now we can calculate the scale factor C by

$$C = \frac{\|e\|_E}{\eta_{C=1}} = \left(\frac{a_{\text{ex}}(u,u) - a(u^h,u^h)}{\eta^2_{C=1}} \right)^{\frac{1}{2}} . \tag{6.3}$$

The numerical results in Table 6.1 demonstrate that a reasonable constant can be found.

6.3 Mesh grading and adaptivity; numerical results

In Figure 6.3 the behaviour of the discretization error using various refinement techniques is demonstrated. Corresponding finite element meshes are illustrated in Figure 6.4. The mesh grading discussed here is realized within a radius of 50 around the singular point $(50,0)$, see Figure 6.1. According to Remark 4.4 an appropriate grading parameter employed here is given as $\mu = 0.4$.

With uniform mesh refinement the convergence order depends on the regularity of the exact solution, see Figure 6.3. By refinement new degrees of freedom are created and uniformly distributed over the domain so that neither the structure of the exact solution nor the distribution of the finite

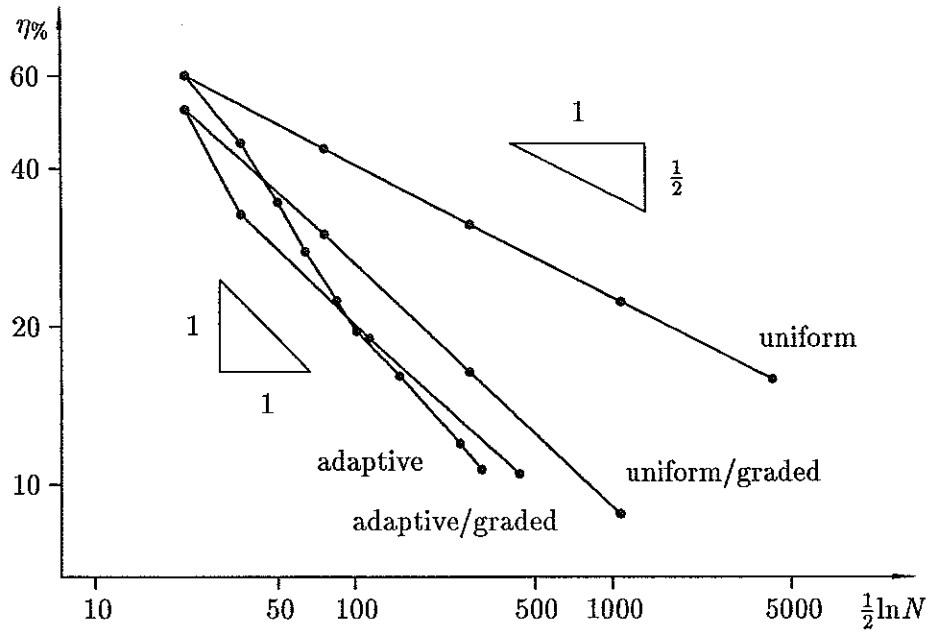

Figure 6.3: Behaviour of the discretization error by using various mesh refinement techniques.

element discretization error is taken into consideration. Therefore with uniform mesh refinement the highest discretization error remains around the singularity. In Figure 6.4(a) the mesh after 3 uniform refinements (1072 degrees of freedom) is shown.

In adaptive techniques the influence of the singularity on the convergence order is eliminated. Controlled by local error indicators a mesh refinement is produced especially near the singularity. We reach a global convergence order of approximately one, which is optimal for finite element approximations with linear shape functions. With classical adaptive techniques, however, the mesh refinement is *locally uniform*, i. e. an element which has to be refined is divided in four congruent subelements. Information about localisation and order of singularities to control *a-priori* a graded mesh design are not included. Therefore usually a large number of refinement steps are needed to achieve a sufficiently fine mesh around the singular point.

The uniform mesh refinement with mesh grading leads to the same optimal convergence order as in the case of adaptive refinement. By an appropriate mesh grading of the uniform refined mesh the influence of the singularity on the convergence order of the finite element solution is eliminated. Notice,

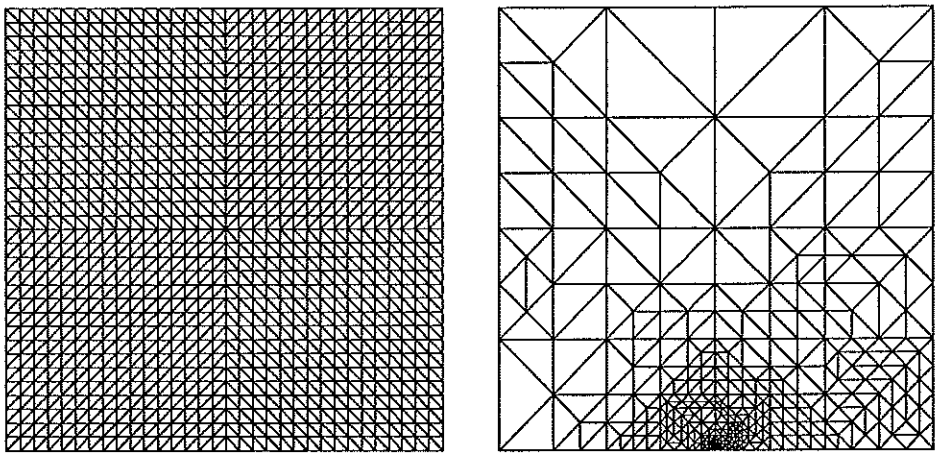

(a) uniform

(b) adaptive

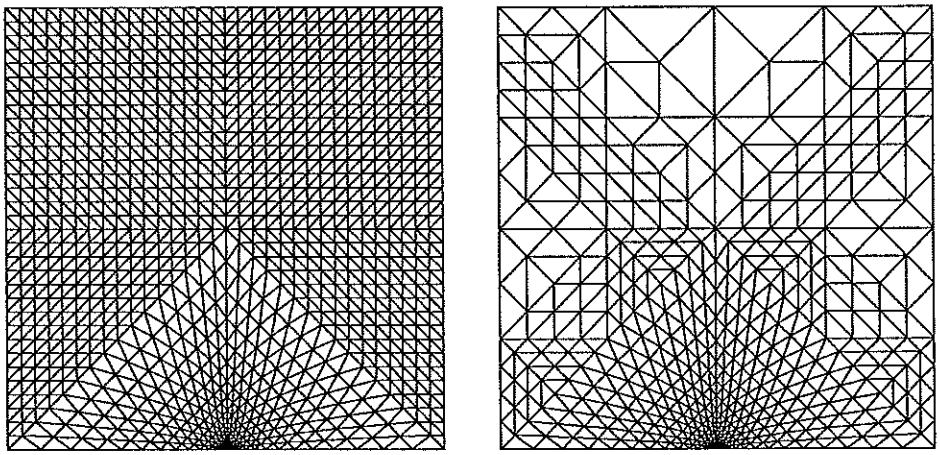

(c) uniform with grading

(d) adaptive with grading

Figure 6.4: Finite element meshes after various refinement strategies.

that in the initial mesh a mesh grading already reduces the discretization error from 60.20% to 51.93%, see Figure 6.3.

The most efficient mesh refinement technique is obviously the adaptive mesh refinement combined with mesh grading around the singularity. The convengence order achieved is near one which has already been obtained with uniform graded refinement as well as with classical adaptive refinement. In comparison with uniform graded refinement, however, the error level expressed by the constant C^* in (3.7) is now decreased. In contrast to classical adaptive refinement the number of meshes needed to achieve a certain error level is substantially reduced. A further simple comparision shows the advantage of adaptive graded refinement techniques: Whilst with an adaptive graded mesh the error level of about 10% is reached after 3 refinements employing finally 437 degrees of freedom, we would obtain the same error level with uniform ungraded mesh refinement with about 27000 degrees of freedom (result extrapolated).

7 Tests in a three-dimensional domain

7.1 The numerical example

In the three-dimensional domain

$$\Omega = \{(x_1, x_2, x_3) = (r\cos\varphi, r\sin\varphi, z) \in \mathrm{R}^3 : r < 1, 0 < \varphi < \frac{3}{2}\pi, 0 < z < 1\}$$

we consider *Laplace*'s equation with essential boundary conditions

$$\Delta u = 0 \quad \text{in } \Omega, \tag{7.1}$$

$$u = \overline{u} \quad \text{on } \partial\Omega. \tag{7.2}$$

The right hand side $\overline{u}$ is taken such that

$$u = (10 + z)r^{2/3}\sin\frac{2}{3}\varphi \tag{7.3}$$

is the exact solution of the problem which has the typical singular behaviour at the edge.

7.2 Uniform mesh refinement with grading

First we investigate the influence of mesh grading on the behaviour of the finite element error, and especially on the convergence order of the error.

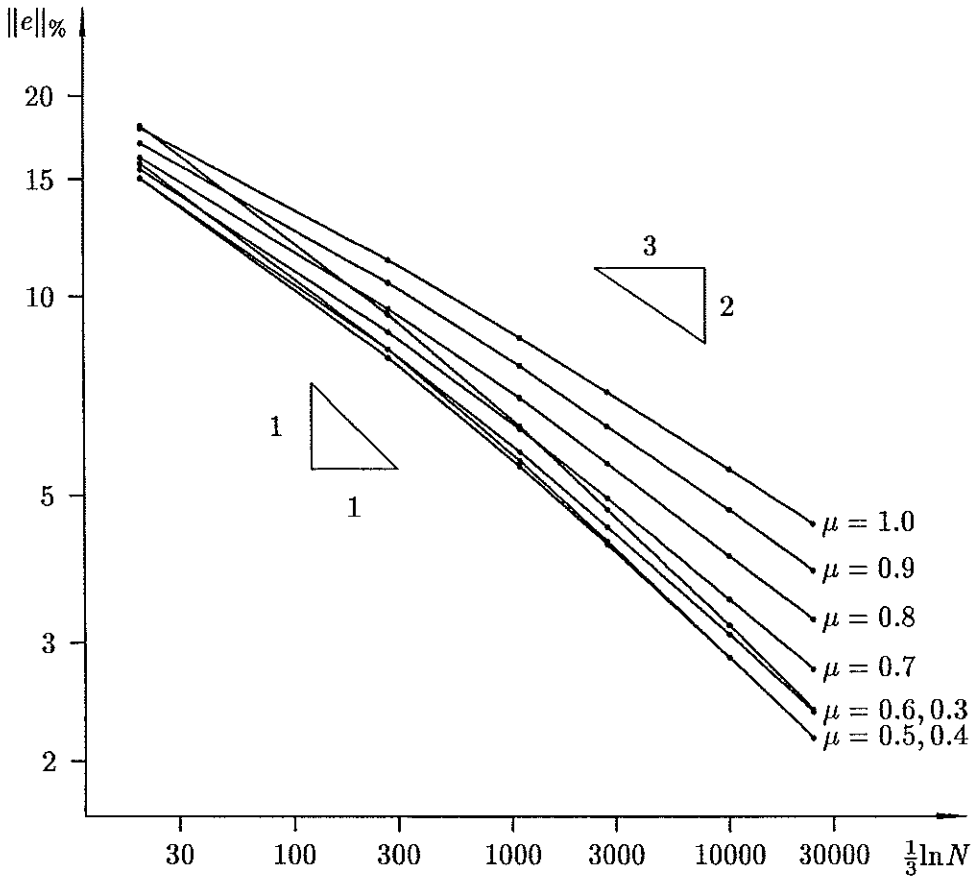

Figure 7.1: Behaviour of the error for different grading parameters μ.

Anisotropic meshes are constructed by a transformation of the ungraded meshes, as described in Section 4, see Figure 4.3. We vary the number of element layers M (6, 9, 12, 18, 24) and the grading parameter μ (1.0, 0.9, ...). From the numerical solution the energy norm $\|e\|_E$ of the finite element error $e = u - u^h$ is computed by numerical integration with a 14-point-formula. As in the previous section, these norms are arranged in a double logarithmic scale in Figure 7.1. We can observe that the error is decreasing with decreasing values of μ until some optimal μ_* of about 0.5, then it increases again. Note also that $\mu = 0.4$ and $\mu = 0.3$ give a relatively large error for coarse meshes.

The convergence order is increasing with decreasing μ, but is still not in its asymptotic range. (There are relatively large differences among the calculated approximation orders with respect to the number of degrees of freedom, the number of nodes and the number of elements, though they should be asymtotically the same. The reason for this is the relatively large proportion (about 20%) of boundary nodes, which have no degrees of freedom.)

We can conclude that the anisotropic, graded meshes are useful for treating edge singularities, for diminishing the error and achieving the optimal approximation order.

7.3 Error estimation

In addition to the computation of the error norm $\|e\|_E$ using the exact solution, we estimate the errors with the error estimator described in Section 5. As in Section 6 the indicator λ_i reduces to

$$\lambda_i^2 = C^2 h_i \int_{\partial\Omega_i} \overline{J}^2 d\Gamma = C^2 \sum_{j=1}^{4} h_{ij} \int_{(\partial\Omega_i)_j} \overline{J}^2 d\Gamma, \tag{7.4}$$

where the domains $(\partial\Omega_i)_j$ denote now the faces of the tetrahedron Ω_i. In two variants, the discretization parameter h_{ij} is taken at first related to the areas of the faces,

$$h_{ij} = (2\,\mathrm{meas}((\partial\Omega_i)_j))^{1/2}, \tag{7.5}$$

and at second related to the volume of the element,

$$h_{ij} = (6\,\mathrm{meas}(\Omega_i))^{1/3}. \tag{7.6}$$

			h_{ij} as in (7.5)		h_{ij} as in (7.6)	
M	N	$\|e\|_E$	$\eta_{C=1}$	$\|e\|_E/\eta_{C=1}$	$\eta_{C=1}$	$\|e\|_E/\eta_{C=1}$
3	20	2.3391	10.5970	0.221	10.4270	0.224
6	275	1.4915	6.7680	0.220	6.6615	0.224
12	2783	0.9444	4.2717	0.221	4.2060	0.225
24	24863	0.5965	2.6912	0.222	2.6504	0.225

Table 7.1: Behaviour of the error estimator for $\mu = 1.0$.

			h_{ij} as in (7.5)		h_{ij} as in (7.6)	
M	N	$\|e\|_E$	$\eta_{C=1}$	$\|e\|_E/\eta_{C=1}$	$\eta_{C=1}$	$\|e\|_E/\eta_{C=1}$
3	20	1.9886	10.5930	0.188	9.9354	0.200
6	275	1.0655	6.1399	0.174	5.6382	0.189
12	2783	0.5562	3.4363	0.162	3.0910	0.180
24	24863	0.2858	1.8775	0.152	1.6555	0.173

Table 7.2: Behaviour of the error estimator for $\mu = 0.5$.

In Table 7.1 and Table 7.2 we set out, for meshes with different numbers M of layers, the exact error norm and the estimates $\eta_{C=1}$ in both variants of the discretization parameter. For ungraded meshes ($\mu = 1.0$) the ratio $\|e\|_E/\eta_{C=1}$ is almost independent of the mesh size, so that extrapolation techniques as described in Subsection 3.2 will give a reasonable constant.

As illustrated in Table 7.2, in uniform graded meshes ($\mu < 1$) the ratio $\|e\|_E/\eta_{C=1}$ changes significantly with the number M of layers. We see the reason for this in the unbounded aspect ratio (Remark 4.1). Note that the aspect ratio is of order $N^{3(-1+1/\mu)}$ for elements near the edge. — A modification of the error estimator is necessary, for example by employing another discretization parameter h_i.

7.4 Adaptive mesh refinement with grading

Because the exact solution of the boundary value problem under investigation is given in (7.3), we can also use the exact error function $e = u - u^h$ to indicate the local discretization error. The adaptive algorithm can be summarized in the following way: Given a tolerance ε that should bound

the global error, we mark all elements Ω_i for which the relation

$$\frac{\|e\|^2_{\Omega_i}}{\text{meas}(\Omega_i)} \leq c\frac{\varepsilon^2}{\text{meas}(\Omega)}, \quad c = 1.5, \tag{7.7}$$

is fulfilled. Then all marked tetrahedra are divided into 8 smaller ones. Finally all elements with irregular nodes are divided such that a regular mesh is produced. We remark that this *green closure* is removed before the next refinement step starts in order to avoid a subsequent division of these elements.

Remark 7.1 Condition (7.7) was derived from the idea that in the final mesh the square of the element error should be proportional to the volume of the element, that means, larger elements should be allowed to have a larger contribution to the total error. Consequently, the ideal case would be

$$\frac{\|e\|^2_{\Omega_i}}{\text{meas}(\Omega_i)} = \frac{\varepsilon^2}{\text{meas}(\Omega)}, \quad \text{for all } i = 1, \ldots, m.$$

If we choose $c = 1$ in (7.7), the final mesh will produce an error strictly below the desired level ε in practical cases. For $c > 1$ these are less elements in which the error is too high. The resulting system of equations is smaller. If c is chosen too large, it is possible that the desired error tolerance will not be achieved though no element violates the test. Our practical experience has shown that $c = 1.5$ is a good choice.

Note also that condition (7.7) implies that in general in each refinement step more elements violate the test when a smaller parameter ε is given. The strategy is not to minimize the error for a given number of degrees of freedom but to try to reach the given error level with as few refinement steps as possible.

In the computational tests, we have varied the grading parameter μ between 0.3 and 0.7, the desired error tolerance between 3% and 10%, as well as the mesh size of the initial mesh. Here we present only the cases $\mu = 0.5$, $\varepsilon = 0.05\,\|u^h\|_E$ and initial meshes like those in the previously described test, but with only $M = 3$, 4 and 5 layers. The results of the other cases are similar. For comparison, we present also the result with $\mu = 1$, that means without grading.

We used two strategies of involving mesh grading. In the first one only the initial mesh was graded. The new nodes introduced in the refinement

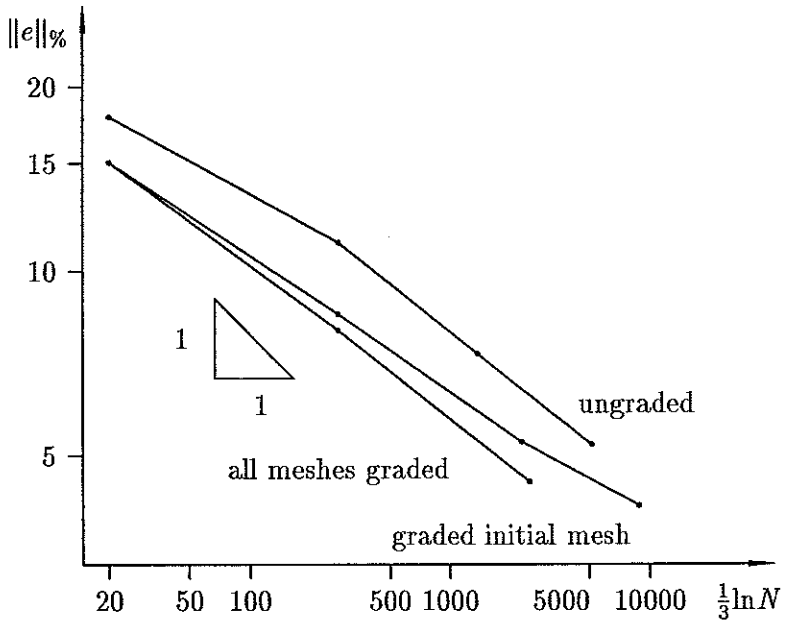

Figure 7.2: Error in the energy norm, initial mesh with 3 layers.

process are generated in the midpoints of the edges of the element of the previous level. The disadvantage of this procedure is that the effect of grading gets partially lost during the refinement process. Obviously it would be an advantage not to start with a too coarse initial mesh.

Our results show this behaviour exactly. For the graded initial mesh with 4 or 5 layers the error is below the tolerance with less degrees of freedom and only 2 refinement steps in comparison to 3 refinement steps in the case without grading, see Figures 7.2 to 7.4 for the different cases.

In a second strategy the refined meshes were also graded. This was realised by two node movements. The first one was executed before the refinement in order to reproduce an ungraded mesh; it is the same transformation with $\frac{1}{\mu}$ instead of μ. The ungraded mesh is then refined, and the grading is produced again. Note that all nodes of the graded mesh have exactly the same coordinates in the next mesh. — Especially for simple geometries as in our cases the movement procedure can be programmed extremely easily. The mesh grading consumes much less time than the refinement step.

The result of this second strategy is a further improvement of the finite element process. Now the error is below the tolerance ε in two refinement steps also for the coarsest initial mesh we used.

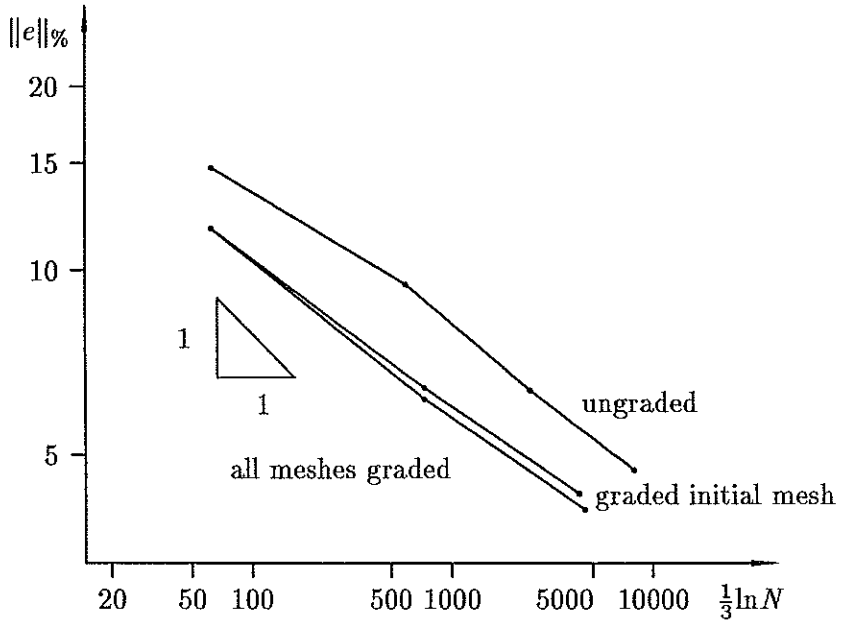

Figure 7.3: Error in the energy norm, initial mesh with 4 layers.

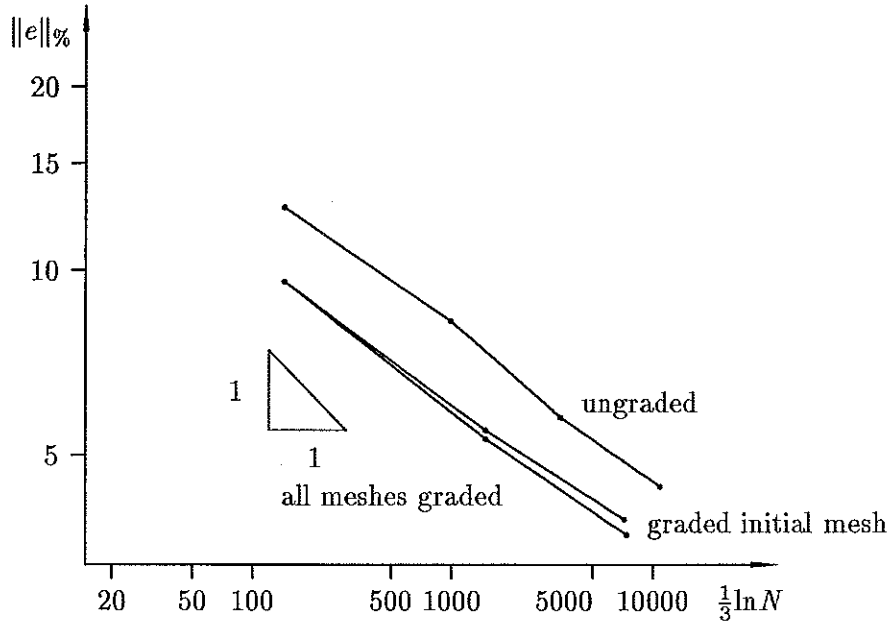

Figure 7.4: Error in the energy norm, initial mesh with 5 layers.

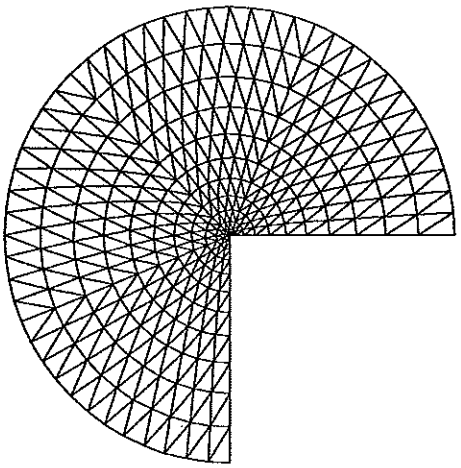

(a) uniform, graded, $M = 12$

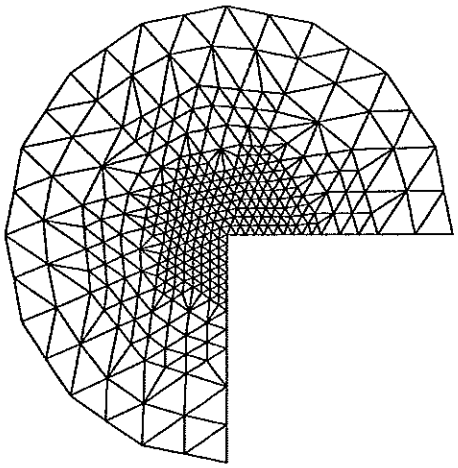

(b) adaptive, without grading

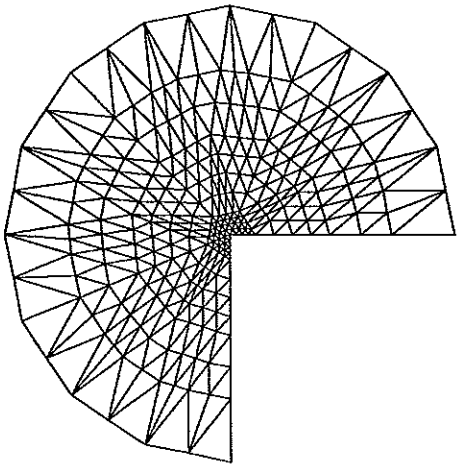

(c) adaptive, graded initial mesh

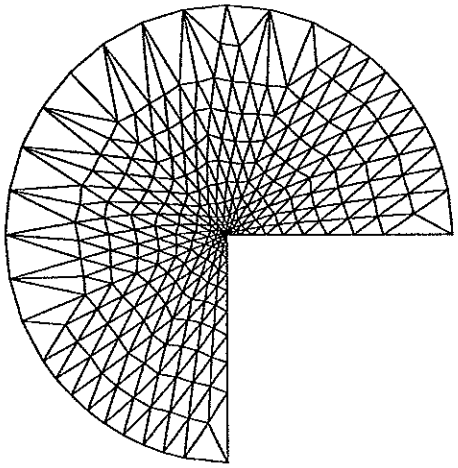

(d) adaptive, all meshes graded

Figure 7.5: Cross-cuts through final meshes at $z = \frac{1}{3}$.

In Figure 7.5 we present cross-cuts through the final meshes at $z = \frac{1}{3}$ for the three cases, in which the initial mesh consists of 3 layers. For comparison we give a uniform, graded mesh with 12 layers.

8 Concluding remarks

The technique of *a-priori* mesh grading around certain singularities has been incorporated successfully into *a-posteriori* mesh refinement strategies. By using an unified *a-priori a-posteriori* approach the advantages of both the grading and the refinement procedures can be combined in order to reduce the local and global discretization error of the finite element solution more rapidly.

The key point in finite element analysis of boundary value problems with singularities is that sufficiently small mesh sizes around singularities become necessary to bring the discretization error under a certain level. In classical adaptive finite element methods, where with each adaptive refinement step the mesh size around the singularity can be decreased at most by one half, usually a large number of steps is needed to achieve the desired error level. Adaptive refinement combined with mesh grading seems to be a suitable tool for improving finite element meshes around singularities faster than without this feature.

References

[1] Th. Apel and M. Dobrowolski, "Anisotropic interpolation with applications to the finite element method," *Computing* **47**, 277–293 (1992).

[2] Th. Apel and B. Heinrich, "Mesh refinement and windowing near edges for some elliptic problem," to appear in *SIAM J. Numer. Anal.*

[3] Th. Apel, A.-M. Sändig, and J.R. Whiteman, "Graded mesh refinement and error estimates for finite element solutions of elliptic boundary value problems in non-smooth domains," in preparation.

[4] A.W. Craig, M. Ainsworth, J.Z. Zhu and O.C. Zienkiewicz, "h and h-p version error estimation and adaptive procedures from theory to practice," *Engineering with Computers* **5**, 221–234 (1989).

[5] L. Demkowicz, J. T. Oden, W. Rachowicz and O. Hardy, "Toward a universal *h-p* adaptive finite element strategy. Part 1: Constrained

approximation and data structure," *Comp. Meth. Appl. Mech. Eng.* **77**, 79–112 (1989).

[6] K. Erikkson and C. Johnson, "An adaptive finite element method for linear elliptic problems," *Mathematics of Computation* **50**, 361–383 (1988).

[7] R. Fritzsch, *Optimale Finite-Elemente-Approximationen für Funktionen mit Singularitäten*, Thesis, TU Dresden, (1990).

[8] R. Fritzsch and P. Oswald, "Zur optimalen Gitterwahl bei Finite-Elemente-Approximationen," *Wiss. Zeitschr. TU Dresden* **37**, 155–158 (1988).

[9] J.P. Gago, D.W. Kelly, O.C. Zienkiewicz and I. Babuška, "A-posteriori error analysis and adaptive processes in the finite element method. Part II: Adaptive processes," *Int. J. Num. Meth. Eng.* **19**, 1621–1656 (1983).

[10] D.W. Kelly, J.P. Gago, O.C. Zienkiewicz and I. Babuška, "A-posteriori error analysis and adaptive processes in the finite element method. Part I: Error analysis", *Int. J. Num. Meth. Eng.* **19**, 1593–1619 (1983).

[11] J.T. Oden, L. Demkowicz, T.A. Westerman and W. Rachowicz, "Toward a universal h-p adaptive finite element strategy. Part 2. A posteriori error estimates," **Comp. Meth. Appl. Mech. Eng. 77**, 113–180 (1989).

[12] W. Rachowicz, J. T. Oden and L. Demkowicz, "Toward a universal *h-p* adaptive finite element strategy. Part 3: Design of *h-p* meshes", *Comp. Meth. Appl. Mech. Eng.* **77**, 181–212 (1989).

[13] B.A. Szabo, "The use of a-priori estimates in engineering computations," *Comp. Meth. Appl. Mech. Eng.* **82**, 139–154 (1990).

[14] O.C. Zienkiewicz and R.L. Taylor, "The finite element method. Fourth edition, Volume 1: Basic formulation and linear problems. Volume 2: Solid and fluid mechanics and non-linearity," *McGraw-Hill Book Company*, 1991.

[15] L.A. Oganesyan and L.A. Rukhovets, *Variational-difference methods for solving elliptic equations* (in Russian), Izdatel'stvo Akad. Nauk Arm. SSR, Jerevan, 1979.

[16] G. Raugel, "Résolution numérique par une méthode d'éléments finis du probléme Dirichlet pour le Laplacien dans un polygone," *C. R. Acad. Sci. Paris, Sér. A* **286**, A791–A794 (1978).

[17] A.H. Schatz and L.B. Wahlbin, "Maximum norm estimates in the finite element method on plane polygonal domains. Part 1," *Mathematics of Computation* **32**, 73–109 (1978).

[18] A.H. Schatz and L.B. Wahlbin, "Maximum norm estimates in the finite element method on plane polygonal domains. Part 1: **32**, 73–109 (1978). Part 2," *Mathematics of Computation* **33**, (465–492) (1979).

[19] I. Babuška and W.C. Rheinboldt, "A-posteriori error estimates for the finite element method," *Int. J. Num. Meth. Eng.* **12**, 1597–1615 (1978).

[20] I. Babuška and W.C. Rheinboldt, "Error estimates for adaptive finite element computations," *SIAM J. Num. Anal.* **15**, 736–754 (1978).

[21] I. Babuška and W.C. Rheinboldt, "On the reliability and optimality of the finite element method," *Comput. Struct.* **10**, 87–94 (1979).

[22] J. Peraire, M. Vahdati, K. Morgan and O.C. Zienkiewicz, "Adaptive remeshing for compressible flow computation", *J. Comp. Phys.* **72**, 449–466 (1987).

[23] T. Strouboulis and K.A. Haque, "Recent experiences with error estimation and adaptivity. Part 1: Review of error estimators for scalar elliptic problems," *Comp. Meth. Appl. Mech. Eng.* **97**, 399–436 (1992).

[24] T. Strouboulis and K.A. Haque, "Recent experiences with error estimation and adaptivity. Part 2: Error estimation for h-adaptive approximations on grids of triangles and quadrilaterals," *Comp. Meth. Appl. Mech. Eng.* **100**, 359–430 (1992).

[25] P. Grisvard, *Elliptic problems in nonsmooth domains*, Pitman, Boston, 1985.

[26] E. Rank, M. Schweingruber and M. Sommer, "Adaptive mesh generation and transformation of triangular to quadrilateral meshes", *Comm. Num. Meth. Eng.* **9**, 121–129 (1993).

[27] E. Rank and O.C. Zienkiewicz, "A simple error estimator in the finite element method," *Comm. Appl. Num. Meth.* **3**, 243–249 (1987).

[28] A. Kufner and A.-M. Sändig, *Some applications of weighted Sobolev spaces*, BSG B. G. Teubner Verlagsgesellschaft, Leipzig, 1987.

[29] I. Babuška and B.A. Szabo, "On the rates of convergence of the finite element method," *Int. J. Num. Meth. Eng.* **18**, 323–343 (1982).

[30] L.A. Oganesyan and L.A. Rukhovets, "On variational-difference methods for linear elliptic equations of second order in two-dimensional domains with piecewise smooth boundary (in Russian)," *Zh. Vytcheslit. Math. Math. Fiz.* **8**, 97–114 (1968).

[31] I. Babuška and W. Gui, "Basic principles of feedback and adaptive approaches in the finite element method," *Comp. Meth. Appl. Mech. Eng.* **55**, 27–42 (1986).

[32] I. Babuška and A. Miller, "A feedback finite element method with a-posteriori error estimation. Part I: The finite element method and some basic properties of the a-posteriori error estimates," *Comp. Meth. Appl. Mech. Eng.* **61**, 1–40 (1987).

[33] M. Ainsworth, J.Z. Zhu, A. W. Craig and O. C. Zienkiewicz, "Analysis of the Zienkiewicz-Zhu a-posteriori error estimator in the finite element method," *Int. J. Num. Meth. Eng.* **28**, 2161–2174 (1989).

[34] J.Z. Zhu and O.C. Zienkiewicz, "Superconvergence recovery technique and a posteriori error estimators," *Int. J. Num. Meth. Eng.* **30**, 1321–1339 (1990).

[35] O.C. Zienkiewicz, W.D. Kelly, J.P. Gago and I. Babuška, "Hierarchical finite element approaches, error estimate and adaptive refinement," in *The Mathematics of Finite Elements and Applications IV. Mafelap 1981*, J.R. Whiteman, Ed., Academic Press, 1982, p. 313–346.

[36] O.C. Zienkiewicz and J.Z. Zhu, "A simple error estimator and adaptive procedure for practical engineering analysis," *Int. J. Num. Meth. Eng.* **24**, 337–357 (1987).

[37] O.C. Zienkiewicz and J.Z. Zhu, "The superconvergent patch recovery and a-posteriori error estimates. Part 1: The recovery technique," *Int. J. Num. Meth. Eng.* **33**, 1331–1364 (1992).

[38] O.C. Zienkiewicz and J.Z. Zhu, "The superconvergent patch recovery and a-posteriori error estimates. Part 2: Error estimates and adaptivity," *Int. J. Num. Meth. Eng.* **33**, 1365–1382 (1992).

[39] D.W. Kelly, "The self-equilibration of residuals and complementary a-posteriori error estimation in the finite element method," *Int. J. Num. Meth. Eng.* **20**, 1491–1506 (1984).

[40] D.W. Kelly, "The self-equilibration of residuals and 'upper-bound' error estimates for the finite element method", in *Accuracy estimates and adaptive refinements in finite element analysis*, I. Babuška, O.C. Zienkiewicz, J.P. Gago and E.R. Oliveira, Eds., John Wiley & Sons, 1986.